PHYSICAL REVIEW D VOLUME 44, NUMBER 3 1 AUGUST 1991

Modified soft annihilation model of anomalous dilepton and photon production and its comparison with data

Peter Lichard
Department of Theoretical Physics, Comenius University, 842 15 Bratislava, Czechoslovakia

Julia A. Thompson
Department of Physics and Astronomy, University of Pittsburgh, Pittsburgh, Pennsylvania 15260

(Received 25 October 1990; revised manuscript received 15 February 1991)

The soft annihilation model of the production of anomalous prompt photons and dileptons in multiparticle production processes is modified by the inclusion of a gluon component in the intermediate parton state, improving the agreement with data.

I. INTRODUCTION

Since 1966 a number of experiments at different center-of-mass energies and with different projectile-target combinations have reported an excess of lepton pairs, single leptons, and real photons, compared to those expected from bremsstrahlung and decays of known particles. For phenomena above 50 MeV/c transverse momentum, broad qualitative success in explaining these excess particles was seen by the soft annihilation model, based on an idea suggested by Bjorken and Weisberg,[1] and worked out in detail by one of us (P.L.) in collaboration with Černý and Pišút.[2,3] In this model, both lepton pairs and single leptons arise from decay of virtual photons. The virtual photons, in turn, arise in an intermediate state of the reaction by annihilation of quarks and antiquarks produced in the initial stages of the reaction. The parameters of the quark-antiquark system are fixed (in a model-dependent way) by data on the production of hadrons, which, within the context of the model,[4,5] arise from the recombination of produced quarks and antiquarks.

However, quantitative disagreements remained between the soft annihilation calculations and the experimental data. The data are systematically softer in shape than the model calculations. While there are substantial uncertainties[6,7] in the soft photon and lepton data due to a variety of systematic experimental effects, particularly including uncertainties in the production of η's and π's, the data presented to date agree on a soft excess in the central region of the interaction. Three major experiments (DLS at LBL, RISK at Serpukhov, and HELIOS at the CERN SPS) have collected large data samples recently. Some early results are already available from DLS,[8–10] from RISK,[11,12] and from HELIOS.[13–19] Final results, including careful studies of systematic uncertainties, should be available soon. Because of the delicate nature of the systematic uncertainty studies, in this paper we compare the model calculations only to published data.

The forthcoming new results, with their promise of careful studies of systematic errors, provide a motivation to review and understand the apparent discrepancies between the soft annihilation model calculations and the data. If the soft lepton and photon data are reliable and the discrepancies with the soft annihilation model are significant, what physics modifications of the model are required to accommodate the softer shape of the data? The present work offers one answer to this question, the addition of a gluon component to the produced intermediate state partons. The importance of such a gluon component in the intermediate parton state has recently also been advocated by Van Hove in the context of a cold quark-gluon plasma.[20] The size of the component chosen for the present work, based on a rough comparison of model results with the data of one experiment,[21] is equal to the size of the quark $(q + \bar{q})$ component in the sea. The size of this gluon component cannot be inferred from the multiparticle production, since we do not presently have a mechanism for including gluons in the recombination processes which lead to the production of hadrons. Coincidentally, the gluon component we have chosen is the same as that used in a very soft (p_T below 50 MeV/c) photon production study[22] based on Van Hove's cold quark-gluon plasma ideas.

The purpose of the present paper is simply to point out the consequences of an intermediate state gluon component for the soft dilepton and photon production. We shall not aim at a detailed fit to all accessible soft photon and lepton data. Also, the consequences for hadron production of introducing a gluon component may be interesting to explore separately, but they are beyond the scope of the present work.

Neither the soft annihilation model nor the modified soft annihilation model have been derived from QCD. They should be viewed rather as phenomenological tools to look for common features of different pieces of data and to interpolate or extrapolate over different center of mass energy ranges or from p-p to p-A and A-A collisions.[23] Such a phenomenological description of a wide range of data aids in the search for common underlying mechanisms and the appearance of new phenomena which are above results expected by the model extrapolation (for example, an onset of phenomena related to a quark-gluon plasma formation at definite energies or for definite projectile combinations in relativistic heavy-ion collisions[24-28]).

Section II describes the soft annihilation model (SAM) and its modification (MSAM). Section III gives comparisons to presently published data and predictions for experiments in progress.

II. THE ORIGINAL SOFT ANNIHILATION MODEL AND ITS MODIFICATION

A. Original soft annihilation model (SAM)

First we present briefly, for convenience, the basic ideas and relevant formulas of the soft annihilation model. It is assumed that in the course of the collision an intermediate system consisting of quarks and antiquarks is formed. During the existence of this system, quarks and antiquarks have a chance to annihilate, producing photons and dileptons. The correct description of the space-time evolution of the intermediate parton system has been shown[2] to be of the utmost importance for preventing a copious production of high-mass dileptons, because this evolution does not allow annihilation of quarks and antiquarks separated by large rapidity intervals. The mean number of photons (dileptons) per inelastic collision is given by the formula

$$\langle n\rangle = \frac{t_0}{V_0}\sum_{Q,\overline{Q}}\int\cdots\int dy_1\,dy_2\,d^2p_{T_1}\,d^2p_{T_2}\,F_{Q\overline{Q}}(y_1,\mathbf{p}_{T_1},y_2,\mathbf{p}_{T_2})|\mathbf{v}_Q-\mathbf{v}_{\overline{Q}}|\,\sigma_A^Q(y_1,\mathbf{p}_{T_1},y_2,\mathbf{p}_{T_2})\cosh y_1\cosh y_2\,w(y_1,y_2), \tag{1}$$

where t_0 (V_0) is the lifetime (volume) of the intermediate parton system in its rest frame, $F_{Q\overline{Q}}$ is the joint distribution function of quarks and antiquarks, σ_A^Q is the annihilation cross section and $w(y_1,y_2)$ gives the probability of simultaneous excitation of different rapidity. regions[2,3] In SAM it is assumed that the parton distribution function is governed by longitudinal phase space with a transverse-momentum cutoff modified by a factor which pushes valence quarks to the ends of the rapidity plot and by a factor which regulates the relative weight of configurations with different numbers of partons. For the differential probability of the intermediate system with V valence quarks being within an infinitesimal region of N-parton phase space, we thus write

$$dP_N = kG^N\,\delta\left(\sum_{i=1}^N\mathbf{p}_i\right)\delta\left(\sum_{i=1}^N E_i-\sqrt{s}\right)\,V(x_1,\cdots,x_V)\exp\left(-\sum_{i=1}^V p_{T_i}^2/R_{\rm val}^2-\sum_{i=V+1}^N p_{T_i}^2/R_{\rm sea}^2\right)\prod_{i=1}^N dy_i\,d^2p_{T_i}, \tag{2}$$

where

$$V(x_1,\ldots,x_T,x_{T+1},\ldots,x_V)=\prod_{i=1}^T\sqrt{-x_i}\prod_{i=T+1}^V\sqrt{x_i} \tag{3}$$

is the Kuti-Weisskopf factor[29] which gives larger probability to configurations in which valence quarks keep a large momentum fraction x (indices $1,\ldots,T$ refer to valence quarks in the target, $T+1,\ldots,V$ to those in the projectile). The normalization constant k is fixed by the condition

$$1=\sum_{N=V}^{N_M}\int dP_N. \tag{4}$$

The sum extends up to the value N_M at which the individual term contribution is found to be negligible (in the actual calculation we used 10^{-6} as a criterion). The flavor of sea $q\overline{q}$ pairs was generated at random, with probability $(1-\lambda)/2$ for a $u\overline{u}$ or $d\overline{d}$ pair, and probability λ of an $s\overline{s}$ pair. No correlations were introduced in momentum space between members of a given pair.

The form (2) of the probability density and the values of parameters entering it was motivated by the studies[4,5] of multiparticle production. The parameters $R_{\rm sea}$=0.50 and $R_{\rm val}$=0.80 were kept fixed at all energies, whereas G was determined at each energy by requiring that the average charged hadronic multiplicity be consistent with data. The values of G obtained and the corresponding average quark multiplicities are shown in Table I. The quark multiplicities are included because they are used to fix the value of G in the modification of the SAM (the MSAM), which is the subject of this paper and is described in more detail in the following subsection. The remaining parameter λ from the recombination model[4,5] of multiparticle production was introduced above and is taken to be 0.5. It regulates the suppression of $s\overline{s}$ pairs against $u\overline{u}$ (or $d\overline{d}$) ones. Further suppression comes from dynamical effects (higher mass of strange quarks).

After inserting the double distribution functions in-

TABLE I. The values of the energy- and process-dependent parameter G used in the SAM and MSAM calculations. Mean quark multiplicities $n = \langle n_q + n_{\bar{q}} \rangle$ are also shown.

Reaction	W (GeV)	n	G SAM	G MSAM
pN	3.6	7.1	1.60	3.00
πp	5.6	8.5	1.52	2.70
πp	8.5	10.4	1.14	2.00
μp	13.9	13.3	0.82	1.65
pN	20.6	14.9	0.67	1.08
pN	29.1	16.8	0.56	0.88
pp	63.0	21.0	0.41	0.63

duced by (2) into (1) and expressing the annihilation cross section σ_A^Q by means of the cross section for annihilation in head-on collisions of the ith and jth parton $\sigma_{ij}(\hat{s}_{ij})$ we obtain the formula

$$\langle n \rangle = \frac{t_0}{V_0} \sum_{N=V}^{N_M} \sum_{i=2}^{N} \sum_{j<i} \int \frac{\sqrt{(p_i \cdot p_j)^2 - m_i^2 m_j^2}}{m_{T_i} m_{T_j}} \times \sigma_{ij}(\hat{s}_{ij})\, w(y_i, y_j)\, dP_N , \tag{5}$$

with the σ_{ij} equal to zero if the flavors of the ith and jth parton do not allow their annihilation. Equation (5) is the starting point for all SAM calculations. If the distribution of photons or dileptons in some variable(s) is to be calculated, the appropriate δ function(s) should be inserted under the integration sign in Eq. (5) and/or the cross section for the elementary subprocess should be replaced by the corresponding differential quantity. Because the actual calculations were performed by the Monte Carlo method proposed by Jadach,[30] the above mentioned δ function(s) were replaced by step functions for finite bins, and the distributions were obtained in histogram form.

The ratio t_0/V_0 was fixed, in accordance with earlier work,[31] at a value of 3 fm^{-2}. We note, however, that our t_0/V_0 is three times larger than the parameter κ in that work, because a factor 1/3 related to averaging over colors of quarks and antiquarks in the initial state was ignored there.

The model[4,5] was originally designed for describing multiparticle production in hadron-hadron collisions, but a later work[32] has shown that it can also be applied to deep inelastic scattering (DIS). Therefore we assume here also that the SAM (designed originally for hadronic collisions[2,3,31]) can be used to calculate photon and dilepton production in DIS. In fact, the SAM was used even earlier[33] for estimating the soft dimuon yield in DIS, where it leads to the production of trimuons with a small mass unlike pair component, as has been observed.[34]

To illustrate the difficulty with the soft annihilation model in its original version, we present in Figs. 3 and 4

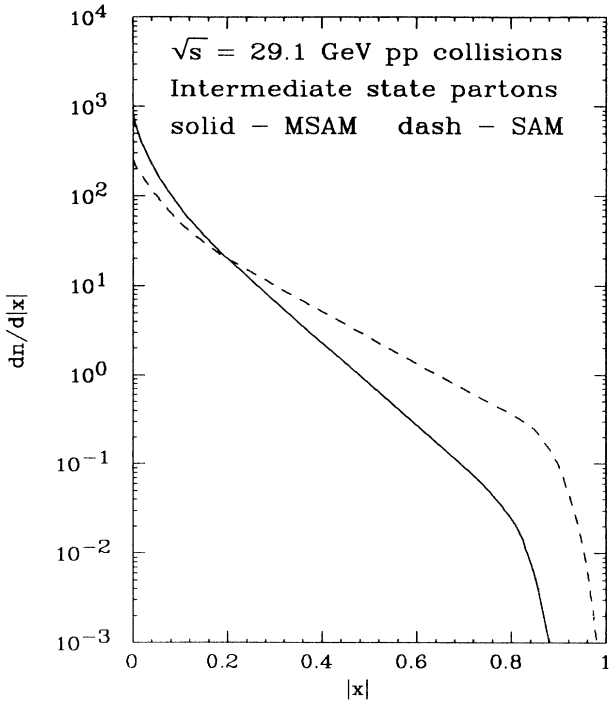

FIG. 1. Inclusive x distribution of partons in the intermediate system in proton-proton collisions at center-of-mass energy 29.1 GeV.

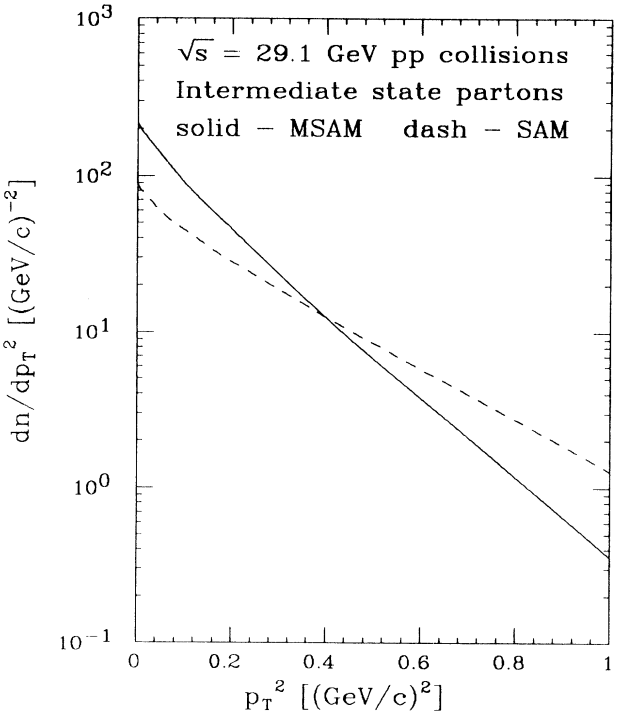

FIG. 2. Inclusive p_T^2 distribution of partons in the intermediate system in proton-proton collisions at center-of-mass energy 29.1 GeV.

the comparison of SAM calculations (dashed lines) to the p_T^2 and z spectra of photons produced in deep inelastic scattering of muons from a proton target.[21] These SAM calculations were performed along the lines of previous work,[35] but differ from the former in lower statistical errors due to more extensive Monte Carlo simulation. The discrepancy at low p_T^2 is clearly visible in Fig. 3. And in Fig. 4 the calculated z spectrum is seen to fall more slowly than the data (we note that the data points at high z may be attributed to muon bremsstrahlung[21]). A question arises as to whether it is possible to improve the agreement of the SAM with the data by changing the parameters of the SAM, loosening the connection to hadronic production. The results of SAM calculations with the transverse momenta of quarks reduced by choosing $R_{\text{sea}} = R_{\text{val}} = 0.32$ are depicted by the dot-dashed curves in Figs. 3 and 4. The agreement with experimental data in p_T^2 is better, but the discrepancy in the z spectrum is not substantially lessened: in fact the z spectrum becomes slightly harder. This effect may be qualitatively understood as a consequence of the transformation of a part of the transverse motion into longitudinal motion. Thus a more substantial modification, to soften both the p_T^2 and z spectra simultaneously, is required.

It should be noted that the calculation described in the previous paragraph was done only with ν and Q^2 fixed at the average values seen in the experiment (113 GeV and 19 GeV^2, respectively). For an exact comparison with the data, a calculation using the ν and Q^2 distribution from the experimental data would be preferable. If these distributions become available a more detailed comparison can be made also including, for example, the dependence of direct photon production on W, the invariant energy of the hadronic system. The same is true, of course, of the MSAM calculations presented in Sec. III.

B. Modified soft annihilation model (MSAM)

The approach taken by the present work is to add a component of gluons to the produced parton content of the intermediate state. This not only makes the partons softer, but also adds another subprocess, which increases the cross section, in the direction required by the data. In order to show the effect of the introduction of such a gluon component, we have used, somewhat arbitrarily, $R_{\text{sea}} = R_{\text{val}} = 0.45$, with the gluon fraction taken the same as the sea quark $(q + \bar{q})$ content, and the quark content fixed at the same value as in the original SAM. The motivation for this choice of the quark content is an intuitive feeling that the hadron multiplicity is closely connected to the quark and antiquark multiplicity in the intermediate parton system, since after recombination the produced quarks and antiquarks become the valence quarks of outgoing hadrons. The ratio t_0/V_0 was taken the same as in the SAM. The gluon fraction was chosen by a rough comparison with the European Muon Collaboration (EMC) direct photon data.[21] The parameter choices seem rather successful, and sufficient with respect to present data and systematic uncertainties. If the precision of future data should warrant, the size of the gluon component could be extracted by a detailed comparison of the model spectra to the data. It should be noted that in a preliminary version of this paper which appeared in a preprint form,[36] we used a gluon fraction larger by a factor of 2, which matched better the somewhat softer preliminary data of the EMC.[37]

The basic relation of the MSAM is formally the same as for the SAM [Eq. (5)]; the only difference is that interactions of gluons with quarks and antiquarks are included in the case of the modified soft annihilation model. The corresponding cross sections for photon and dilepton production subprocesses are given in the Appendix.

To illustrate the softening of parton distribution functions by inclusion of a gluon component, we present the inclusive distribution functions in $x = 2p_L/\sqrt{s}$ (Fig. 1) and p_T^2 (Fig. 2) of partons in the intermediate state created in pp collisions at $\sqrt{s}$=29.1 GeV, calculated on the basis of the formula

$$\frac{dn}{d^3p} = \sum_{N=V}^{N_M} \sum_{i=1}^{N} \int \delta(\mathbf{p} - \mathbf{p}_i)\, dP_N \tag{6}$$

in both SAM and MSAM. It should be stressed that these distributions are only for illustrative purposes. The dilepton production calculation is based directly on Eq. (5) and therefore takes into account correlations among partons. These correlations would not be included if, instead, we used Eq. (1) with the double distribution function written as a product of single parton distribution functions.

III. MSAM RESULTS AND COMPARISON TO DATA

Table II shows the experiments for which MSAM and SAM results are presented and compared.

The data from the EMC experiment,[21] shown in Figs. 3 and 4, give an example of the difference between the SAM and MSAM, and the effect on the SAM of a softening of the quark transverse momentum spectra. The SAM results fall systematically below the observed photons, both at low z and low transverse momentum. The MSAM results have a different shape both in transverse momentum and z, both quantitatively and qualitatively in better accord with the low p_T, low z excess.

Figure 5 shows the single direct central positron production from the CERN ISR in pp collisions at 63 GeV center-of-mass energy.[38–40] For the model calculation we assume that the single electrons are members of a pair. As was done with the experimental data, we require the mass of the pair to be greater than 100 MeV/c^2. Within the large systematic errors of the low-transverse-momentum data, the SAM calculations are able to explain the data, but the MSAM results better reproduce the shape and magnitude of the actual reported values. The result is sensitive to the exact position and efficiency

TABLE II. Experiments compared to SAM and MSAM.

Experiment	Reaction	Accelerator	Energy (GeV) (c.m. or beam)	Particle(s)	Dist.
EMC [21]	μ-p	CERN SPS	200 (beam)	photon	p_T, z
C-P II[45]	p-C	Fermilab	225 (beam)	$\mu^+\mu^-$	M
LASS [43,44]	π-p	SLAC	16 (beam)	e^+e^-	p_T
MPS [49,50]	π-p	BNL	17 (beam)	e^+e^-	x_F
DLS [8,9]	p-Be	LBL	T_{beam}=1–4.9	e^+e^-	M
AFS [38]	p-p	CERN ISR	63 (c.m.)	e^+	p_T
RISK[11]	p-C	Serpukhov	38 (beam)	$\mu^+\mu^-$	x_F, M
HELIOS[55]	p-Be	CERN SPS	450 (beam)	e^+e^-	p_T

of the mass cut. Allowing the inclusion of 20% of the pairs with masses less than 100 MeV/c^2 would raise the MSAM calculation to the level of the data. The recent observation of a branching ratio for $\rho \rightarrow \pi^+\pi^-\gamma$, of more than 1% by the Novosibirsk group[41] raises the question of a contribution to the dielectron spectrum from $\rho \rightarrow \pi^+\pi^-e^+e^-$. Evaluation of this decay mode, along the lines used by Singer[42] for the $\rho \rightarrow \pi^+\pi^-\gamma$ gave a branching ratio of 1.53×10^{-4}. A Monte Carlo simulation confirms that this channel would contribute no more than 1% of the SAM results shown.

Figure 6 gives the SAM and MSAM results for the SLAC pion proton experiment with 16 GeV/c incident pion beams.[43,44] Here the MSAM results better reproduce the low-transverse-momentum points, but the data are above both the SAM and MSAM predictions at larger transverse momenta, more strikingly so for the MSAM results. This may indicate either a residual background from, e.g., η Dalitz decays or a problem with the model, or may simply be a fluctuation in this sample. It will be interesting to see the results of the new experiments.

Figure 7 shows the muon pair mass distribution from the experiment done at Fermilab by the Chicago-Princeton Collaboration.[45,46] The MSAM and SAM contributions for the nuclear case are calculated using an average of proton and neutron targets and extrapolat-

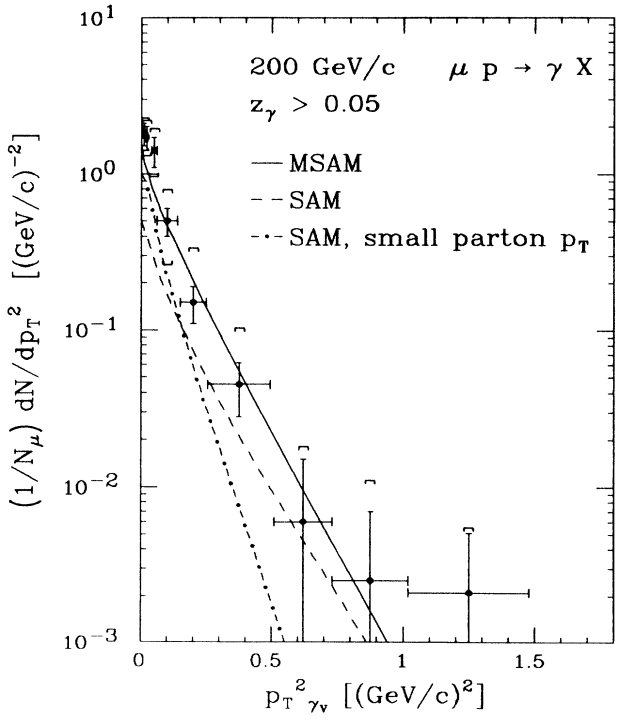

FIG. 3. Direct photon production from EMC: p_T^2 spectrum. The dashed line is the original SAM; the dot-dashed line shows the SAM, modified to give a softer transverse-momentum distribution for the produced quarks. The solid line shows the MSAM results.

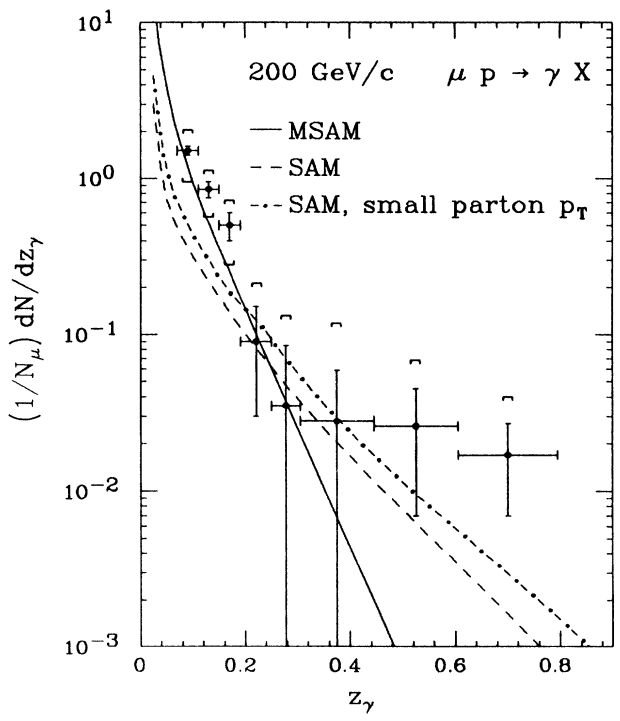

FIG. 4. Direct photon production from the EMC: $z = E_\gamma/\nu$ spectrum. The dashed line is the original SAM; the dot-dashed line shows the SAM, modified to give a softer transverse-momentum distribution for the produced quarks. The solid line shows the MSAM results.

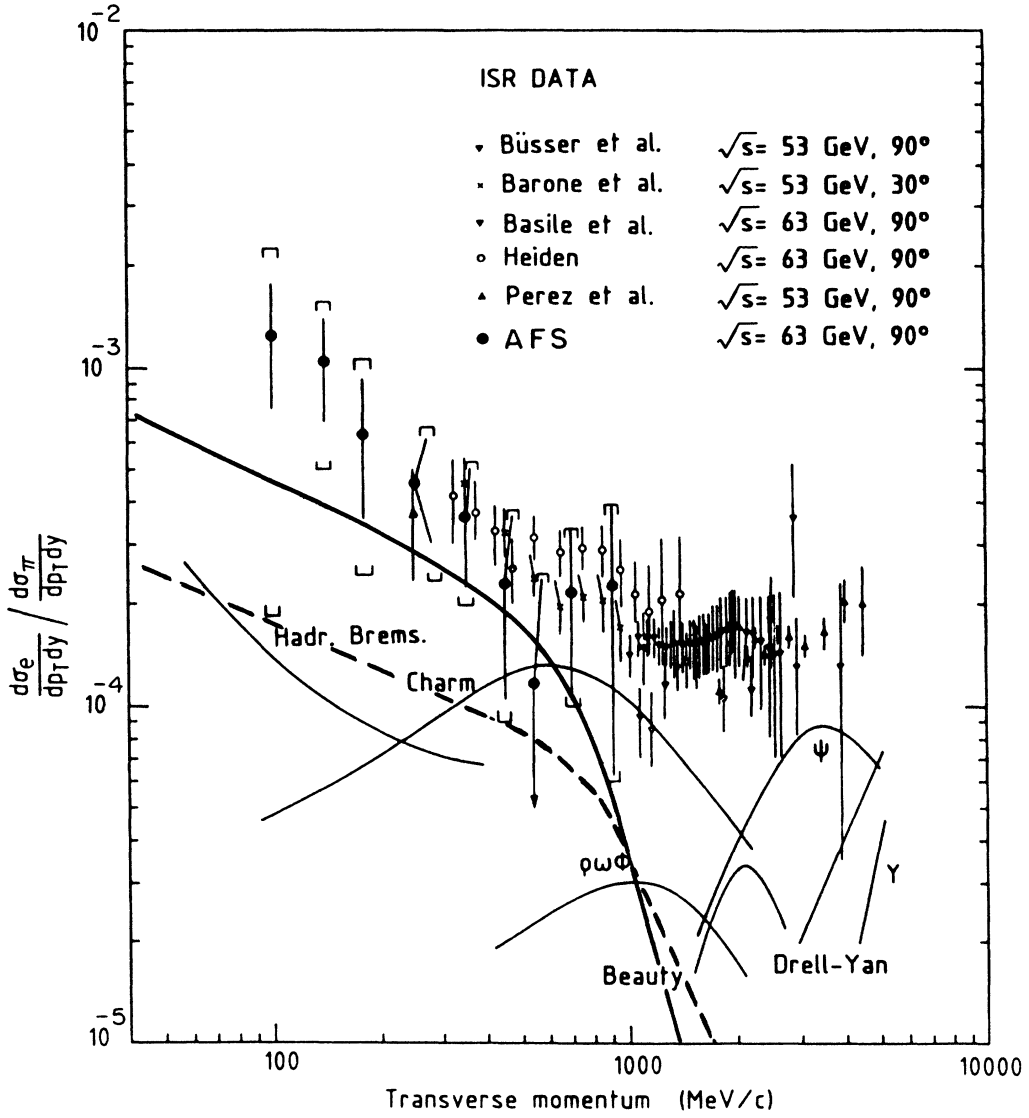

FIG. 5. Direct positron production from the Axial Field Spectrometer (AFS) collaboration: p_T spectrum. Estimated contributions from bremsstrahlung, decays, and the Drell-Yan process are shown as labeled curves, to be summed to give the conventional sources' contribution. The SAM (dashed) and MSAM (solid) predictions are also shown.

ing to the carbon target using an A^α dependence, with α taken to be $0.6 + 0.13M$, based on Figure 3b of the original study.[45] The MSAM contribution is steeper in slope and is also lower in this relatively high mass region than the SAM because of the inclusion of the gluon component. The lower mass data from this collaboration, which would have been somewhat more interesting for this MSAM and SAM comparison, appeared only in a thesis[46] but not in final published form. In addition to the ρ, ϕ, and J/ψ peaks, clearly visible in the data, the contribution from initial-state annihilation (the Drell-Yan process) must be included for complete understanding of the spectrum. Roughly,[47,48] from a copper target the Drell-Yan contribution is about 20% of the continuum at 1 GeV/c^2 and rises to about 90% at M=4 GeV/c^2.

That the anomalous lepton production is a central phenomenon is shown by Fig. 8 and is consistent with the new RISK Collaboration preliminary report[11,12] of little or no excess above x_F of 0.4. Figure 8 shows the x_F distribution for electron pairs from the experiment[49,50] done at BNL and comparisons to the SAM and MSAM. The η and ω background subtraction shown is that used by the experimenters in their original publication, based on a low statistics η and ω production bubble chamber experiment.[51] Measurements at the ISR[52] give a higher value for the η production, by a factor of 3. Use of the higher value for the η production would reduce the

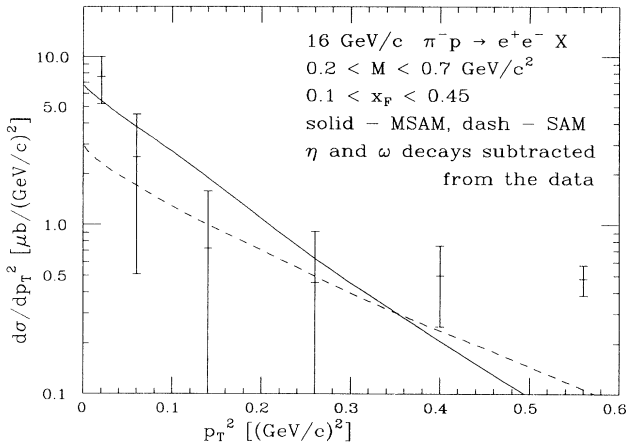

FIG. 6. Direct electron pair production from pion interactions at 16 GeV/c: p_T^2 spectrum. The SAM predictions are the dashed line; the MSAM predictions are the solid line.

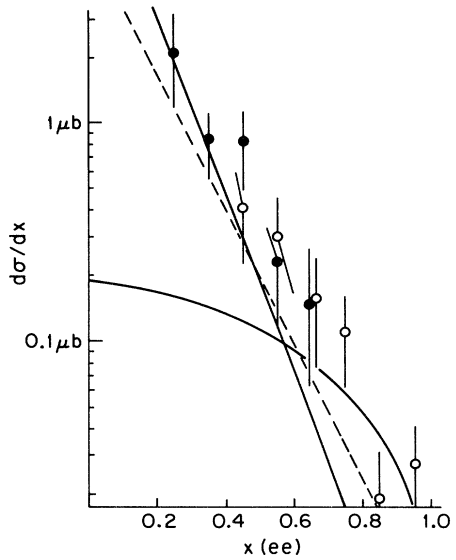

FIG. 8. The x_F distribution for electron pairs from pion-proton interactions at 17 GeV/c incident pion momentum. The background calculated by the experimenters is shown, together with model expectations (SAM, dashed line; MSAM, solid line).

anomalous signal component at high x_F, giving better agreement with the model calculations. The importance of the background subtraction, and its uncertainty in these low center-of-mass energy experiments, emphasizes the importance of the measurement of the η backgrounds in the same experiment which measures the low-mass excess. This important extra control on the systematic errors is present in both the RISK[11,12] and HELIOS[6,7,13–16,19] collaboration experiments, now in the analysis stage, and will facilitate the solid understanding of this signal.

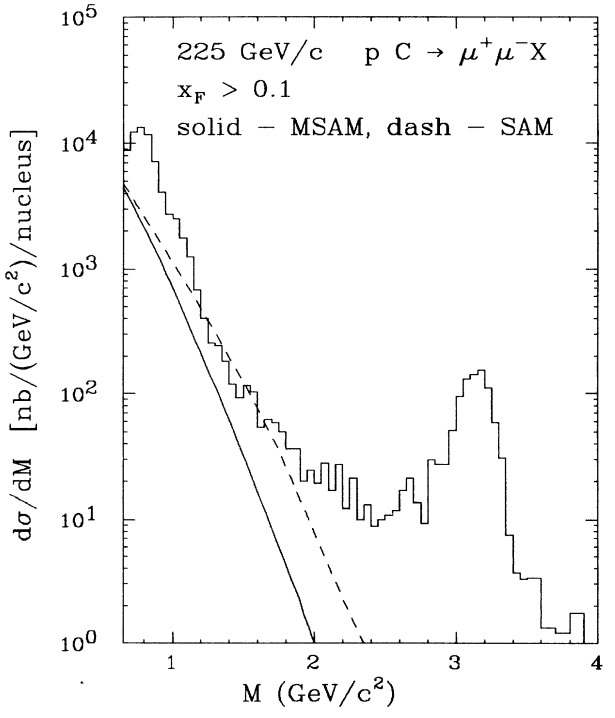

FIG. 7. Direct muon pair production from the Chicago-Princeton experiment: dimuon mass spectrum. The SAM (solid histogram) and MSAM (solid line) predictions are compared with the data. Pairs from the Drell-Yan process may be as much as 1/5 of the data at 1 GeV/c^2.

Table III and Fig. 9 show data from the DLS Collaboration[8,9] from p-Be collisions, with the kinetic energy T of the incident proton ranging from 1.0 to 4.9 GeV. Table III shows the cross section for the produced pairs for three values of T, and Fig. 9 shows the mass spectrum. The data are acceptance corrected, and the dashed line is the decay background presented by the experimenters. As is seen from Table III, the SAM is substantially equivalent to the MSAM. In Fig. 9 we present only the SAM results. There has been discussion in the literature of the variation of the points near the two-pion-mass threshold. The DLS group proposed an explanation based on two pion annihilation,[53] but another calculation[54] found the two-pion annihilation process unable to account for the observed structures. For the mo-

TABLE III. The e^+e^- production cross section per nucleon in the DLS acceptance region and $0.2 < M < 0.7$ GeV/c^2. The "data" are from Fig. 3 of the DLS publication (Ref. 9).

T (GeV)	$\sigma/A_t^{2/3}$ (nb) "Data"	SAM	MSAM
1.0	3.5 ± 1.3	4.9	5.0
2.1	63 ± 11	57	61
4.9	150 ± 20	120	130

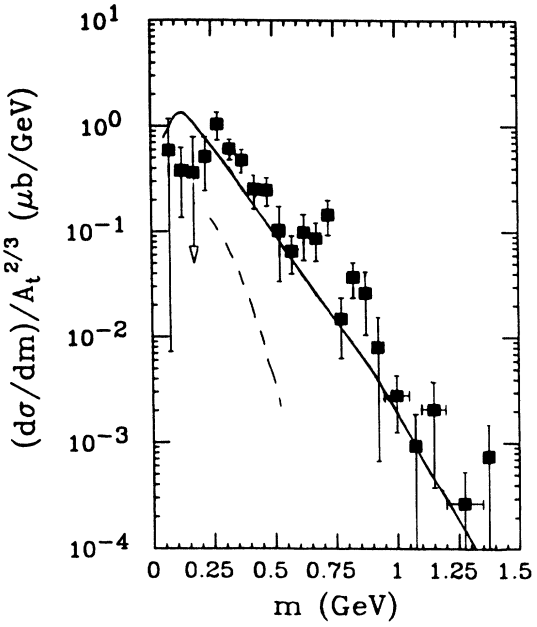

FIG. 9. Mass spectra for electron pairs from the DLS Collaboration. The data are for 4.9 GeV incident proton kinetic energy and are acceptance corrected. The solid line shows the model predictions to be compared with the data. The dashed line shows the expected decay background contributions calculated by the experimenters.

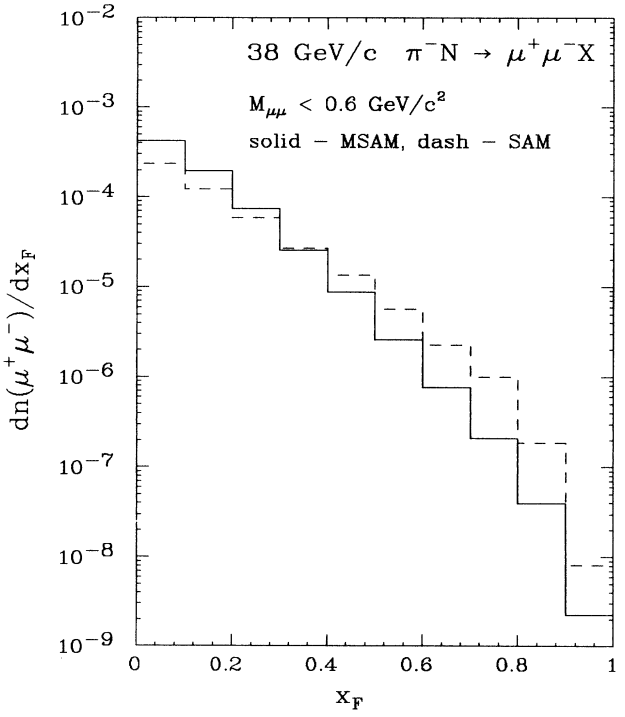

FIG. 10. Predictions for the muon pair spectra in pion-nucleon interactions at 38 GeV/c incident pion momentum, corresponding to forthcoming data from the RISK Collaboration: x_F spectrum. The solid curve shows the MSAM predictions; the dashed curve shows the SAM predictions.

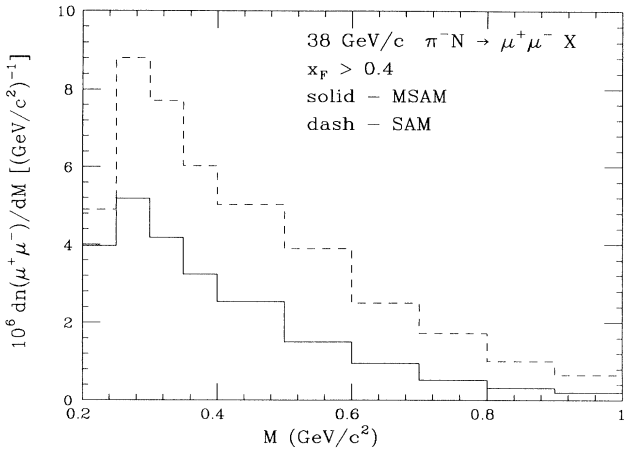

FIG. 11. Predictions for the muon pair spectra in pion-nucleon interactions at 38 GeV/c incident pion momentum, corresponding to forthcoming data from the RISK Collaboration: mass spectrum.

ment, we simply note that the agreement of the DLS data with our calculations is surprisingly good, considering that the average pion multiplicity is quite small, of order 1–2 produced pions.

Figures 10–13 give SAM and MSAM predictions for the large single and dilepton experiments now in the analysis phase. Figures 10 and 11 give predictions for the RISK experiment at Dubna, p-carbon collisions at a beam momentum of 38 GeV/c. Since the MSAM is steeper than the SAM results, the results differ for extrapolation from central rapidities to the region of the RISK acceptance $x_F > 0.4$. The x_F dependence of any signal is thus

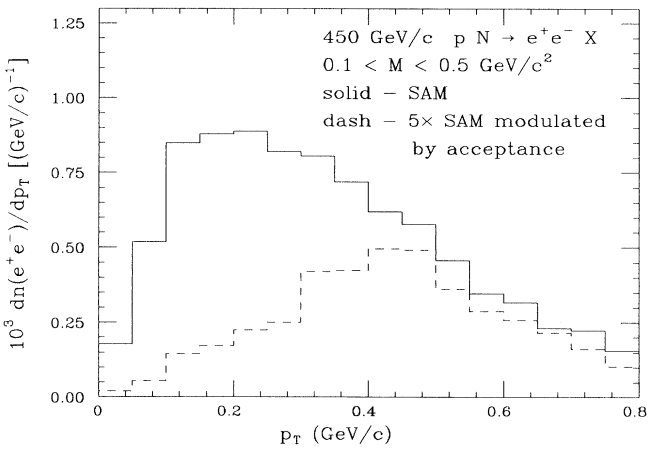

FIG. 12. P_T spectrum predicted by SAM for electron pairs of mass 100–500 MeV/c^2 from p-nucleon collisions at 450 GeV/c incident proton momentum, corresponding to forthcoming data from the HELIOS Collaboration. The solid line is the complete model prediction. The dashed line shows the model weighted by the experimental acceptance and multiplied by a factor of 5 to allow display on the same scale.

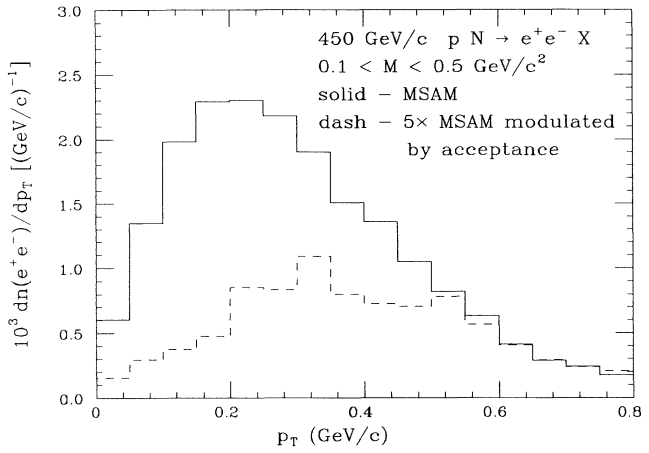

FIG. 13. P_T spectrum predicted from MSAM for lepton pairs of mass 100–500 MeV/c^2 from p-nucleon collisions at 450 GeV/c incident proton momentum, corresponding to forthcoming data from the HELIOS Collaboration. The solid line is the complete model prediction. The dashed line shows the model weighted by the experimental acceptance and multiplied by a factor of 5 to allow display on the same scale.

important as a discriminator between different possible sources for the signal.

Figures 12 and 13 present the model predictions for data from the large HELIOS experiment with data analysis presently in progress. The predictions are shown: (1) directly from the model, and (2) with a set of cuts approximating the HELIOS apparatus, trigger, and analysis cuts:[55,16] both electrons in the range 20–100 mrad; energy of both electrons greater than 2 GeV; and an opening angle of at least 10 mrad between the two electrons. The effect of this approximate set of cuts is shown for illustrative purposes and underestimates somewhat the effective opening-angle cut imposed by the detailed HELIOS analysis.

IV. MULTIPLICITY DEPENDENCE

It has been discussed elsewhere for the SAM[56,23,57] that, in hadronic collisions, because the virtual photons arise from interactions of the quarks in an intermediate state, one expects a faster than linear dependence on associated final state hadronic multiplicity, assuming that the ratio of lifetime to volume (the parameter t_0/V_0) of the intermediate region remains the same. An indication of such behavior has been observed.[40,39] For the photons in μ-p interactions from the EMC this would translate into a dependence on final-state multiplicity for events with fixed W (the hadronic center of mass energy). The same arguments hold for the MSAM.

The study of multiplicity dependence should be seen as a complementary tool to the study of the size and shape of any excess in the mass or other kinematic distributions. Both have their own delicate systematic errors. Multiplicity-dependent biases may destroy or create apparent signal as a function of multiplicity. On the other hand, absolute efficiencies may cancel if one compares the multiplicity dependence of resonant and nonresonant regions. And, if the multiplicity-dependent biases are understood, the comparison of average multiplicities in the signal sample and control events may be useful for small event samples.[23] The combination of the two methods is particularly useful in the case in which the component arising from the intermediate state production may only be comparable to, not much larger than, background processes such as dilepton pairs from meson decays.

V. CONCLUSIONS

In this paper we have discussed the available lepton and photon direct production data for transverse momentum in the range 100–500 MeV/c. In this region the modified soft annihilation model, with an added component of gluons in the intermediate state, gives overall a better description of the available data than the SAM. The calculations affirm that the expected result should be soft and central, in keeping with the recent RISK Collaboration result of only a very small excess in muon pairs for $x_F > 0.4$. Somewhat surprisingly, the MSAM results also give good agreement with recent data on p-Be collisions for 1.0–4.9 GeV incident beam energy. A prediction is given for the HELIOS and RISK experiments from which finished data should be available in the next year.

If the final results from the present large-statistics experiments affirm the previously seen excesses with good statistical precision and systematic reliability, the gluon component in the intermediate state could be extracted from a careful comparison with the experimental data.

ACKNOWLEDGMENTS

Useful discussions with Vlado Černý, Ján Pišút, Jan Böhm, and members of the DLS and HELIOS Collaborations are gratefully acknowledged. One of us (P.L.) particularly wishes to acknowledge the encouragement and interest of the late Léon Van Hove. We thank the DLS Collaboration for supplying us with their acceptance filter computer code. Computer support was provided by the University of Pittsburgh, Ján Ftáčnik, Vlado Černý, and D. E. Kraus. This investigation was initiated during a visit of J.A.T. to Comenius University in conjunction with a scientific exchange visit to the Soviet Union, sponsored by the National Science Academies of the United States and the Soviet Union. Calculations were completed during a visit of P.L. to the University of Pittsburgh. This work was supported in part by the U.S. Department of Energy Grant No. DEAC02-80ER10667.

APPENDIX

We list here the differential cross sections of subprocesses considered in the modified soft annihilation model.

The sum over colors in the final state and averaging over colors in the initial state was performed. s, u, and t are usual Mandelstam variables for the subprocess. The masses of quark, lepton, and dilepton (or virtual photon) are denoted as m, μ, and M, respectively. To make the formulas more transparent we use the following notations:

$$x = \frac{s}{m^2} - 1, \quad y = \frac{t}{m^2} - 1, \qquad z = \frac{u}{m^2} - 1, \quad r = \frac{M^2}{m^2}. \tag{A1}$$

The formulas for real photon production are obtained by putting $M = 0$, those for dileptons by using

$$\frac{d\sigma}{dM^2\,dt} = \frac{d\sigma}{dt} F(M^2) \tag{A2}$$

with

$$F(M^2) = \frac{\alpha}{3\pi} \frac{M^2 + 2\mu^2}{M^4} \sqrt{1 - \frac{4\mu^2}{M^2}}. \tag{A3}$$

We consider the subprocesses:

(1) $q + \overline{q} \longrightarrow \ell^+ + \ell^-$

$$\frac{d\sigma}{d\cos\vartheta} = \frac{\pi}{6s}\alpha^2(\hbar c)^2 \left(\frac{e_q}{e}\right)^2 \sqrt{\frac{s-4\mu^2}{s-4m^2}} \left[1 + \frac{4\left(\mu^2+m^2\right)}{s} + \left(1 - \frac{4\mu^2}{s}\right)\left(1 - \frac{4m^2}{s}\right)\cos^2\vartheta\right], \tag{A4}$$

where ϑ is the angle between quark and lepton momenta in the $q\overline{q}$ rest frame.

(2) $q + \overline{q} \longrightarrow \gamma^* + g$

$$\frac{d\sigma}{dt} = \frac{32\pi}{9}\alpha\alpha_s(\hbar c)^2 \left(\frac{e_q}{e}\right)^2 \frac{1}{s(s-4m^2)} \times \left[\frac{1}{4}\left(\frac{z}{y} + \frac{y}{z}\right) - \left(\frac{1}{y} + \frac{1}{z}\right)^2 - \left(\frac{1}{y} + \frac{1}{z}\right) + \frac{r}{2}\left(\frac{r}{yz} - \frac{1}{y^2} - \frac{1}{z^2} - \frac{1}{y} - \frac{1}{z}\right)\right]. \tag{A5}$$

(3) $g + q \longrightarrow \gamma^* + q$

$$\frac{d\sigma}{dt} = \frac{4\pi}{3}\alpha\alpha_s(\hbar c)^2 \left(\frac{e_q}{e}\right)^2 \frac{1}{(s-m^2)^2} \times \left[\left(\frac{1}{x} + \frac{1}{y}\right)^2 + \frac{1}{x} + \frac{1}{y} - \frac{1}{4}\left(\frac{x}{y} + \frac{y}{x}\right) + \frac{r}{2}\left(\frac{1}{x^2} + \frac{1}{y^2} + \frac{1}{x} + \frac{1}{y} - \frac{r}{xy}\right)\right]. \tag{A6}$$

[1] J. D. Bjorken and H. Weisberg, Phys. Rev. D **13**, 1405 (1976).

[2] V. Černý, P. Lichard, and J. Pišút, Phys. Lett. **70B**, 61 (1977).

[3] V. Černý , P. Lichard, Š. Olejník, and J. Pišút, Acta Phys. Pol. B **10**, 537 (1979).

[4] V. Černý, P. Lichard, and J. Pišút, Phys. Rev. D **16**, 2822 (1977).

[5] V. Černý, P. Lichard, and J. Pišút, Phys. Rev. D **18**, 2409 (1978).

[6] V. Hedberg, seminar at BNL, 1989 (unpublished).

[7] J. A. Thompson, in *Hadron Structure '89*, Proceedings of the Conference, Smolenice, Czechoslovakia, 1989, edited by M. Nagy and D. Krupa (Physics and Applications, Vol. 15) (Slovak Academy of Sciences, Bratislava, 1990), p. 138.

[8] DLS Collaboration, G. Roche *et al.*, Phys. Rev. Lett. **61**, 1069 (1988).

[9] DLS Collaboration, C. Naudet *et al.*, Phys. Rev. Lett. **62**, 2652 (1989).

[10] P. Seidl, in *Soft Lepton Pair and Photon Production*, Proceedings of the Pittsburgh Workshop, edited by Julia A. Thompson (Nova Scientific, Commack, NY, in press).

[11] RISK Collaboration, Dubna Report No. E1-89-486, presented at the International Europhysics Conference on High Energy Physics, Madrid, Spain, 1989 (unpublished).

[12] J. Böhm, in *Soft Lepton Pair and Photon Production* (Ref. 10).

[13] M. J. Clemen, Ph.D. thesis, University of Pittsburgh, 1989.

[14] Y. M. Park, Ph.D. thesis, University of Pittsburgh, 1990.

[15] P. Aubry, Ph.D. thesis, University of Montreal, 1990.

[16] HELIOS Collaboration, P. Nevski, in *Soft Lepton Pair and Photon Production* (Ref. 10).

[17] F. Gibrat-Debu, Ph.D. thesis, Université de Paris VI, 1988.

[18] G. Vasseur, Ph.D. thesis, Centre d'Etudes Nucléaires de Saclay, 1989.

[19] S. Johansson, Ph.D. thesis, University of Lund, 1990; in *Soft Lepton Pair and Photon Production* (Ref. 10).

[20] L. Van Hove, Ann. Phys. (N.Y.) **192**, 66 (1989).

[21] EMC, J. J. Aubert *et al.*, Phys. Lett. B **218**, 248 (1989).

[22] P. Lichard and L. Van Hove, Phys. Lett. B **245**, 605 (1990).

[23]P. Lichard, Z. Phys. C **37**, 125 (1987).
[24]E. V. Shuryak, Phys. Rep. **61**, 71 (1980).
[25]L. D. McLerran and T. Toimela, Phys. Rev. D **31**, 545 (1985).
[26]R. C. Hwa and K. Kajantie, Phys. Rev. D **32**, 1109 (1985).
[27]K. Kajantie, J. Kapusta, L. McLerran, and A. Mekjian, Phys. Rev. D **34**, 2746 (1986).
[28]W. Willis, rapporteur's talk at the Europhysics Conference, Uppsala, Sweden, 1987 (unpublished); in *Panic '87*, Proceedings of the Eleventh International Conference on Particles and Nuclei, 1987, edited by S. Homma *et al.* [Nucl. Phys. **A478**, 151c (1988)].
[29]J. Kuti and V. F. Weisskopf, Phys. Rev. D **4**, 3148 (1970).
[30]S. Jadach, Comput. Phys. Commun. **9**, 297 (1975).
[31]V. Černý, P. Lichard, and J. Pišút, Phys. Rev. D **24**, 652 (1981).
[32]J. Boháčik, A. Nogová, and P. Lichard, Phys. Rev. D **22**, 1212 (1980).
[33]V. Černý, P. Lichard, and J. Pišút, Acta Phys. Pol. B **9**, 269 (1978); Czech. J. Phys. B **29**, 1394 (1979).
[34]B. C. Barish *et al.*, Phys. Rev. Lett. **38**, 577 (1977); T. Hansl *et al.*, Nucl. Phys. **B142**, 381 (1978).
[35]P. Lichard, N. Pišútová, and J. Pišút, Z. Phys. C **42**, 641 (1989).
[36]P. Lichard and J. A. Thompson, Report No. PITT-90-16, 1990 (unpublished).
[37]EMC, J.J Aubert *et al.*, Report No. CERN-EP/88-33, 1988 (unpublished).
[38]T. Åkesson *et al.*, Phys. Lett. B **152**, 411 (1985).
[39]V. Hedberg, Ph.D. thesis, CERN EP Internal Report No. 87-05, 1987.
[40]T. Åkesson *et al.*, Phys. Lett. B **192**, 483 (1987).
[41]I. B. Vasserman *et al.*, Yad. Fiz. **47**, 659 (1988) [Sov. J. Nucl. Phys. **47**, 1035 (1988)].
[42]P. Singer, Phys. Rev. **130**, 2441 (1963); **161**, 1694 (1967).
[43]R. Stroynowski *et al.*, Phys. Lett. **97B**, 315 (1980).
[44]D. Blockus *et al.*, Nucl. Phys. **B201**, 205 (1982).
[45]J. G. Branson *et al.*, Phys. Rev. Lett. **38**, 1334 (1977).
[46]G. G. Henry, Ph.D. thesis, University of Chicago, 1977.
[47]C. Reece *et al.*, Phys. Lett. **85B**, 427 (1979).
[48]D. McCal *et al*, Phys. Lett. **85B**, 432 (1979).
[49]J. Stekas *et al.*, Phys. Rev. Lett. **47**, 1686 (1981).
[50]M. R. Adams *et al.*, Phys. Rev. D **27**, 1977 (1983).
[51]J. Bartke *et al.*, Nucl. Phys. **B118**, 360 (1977).
[52]M. Bourquin and J. M. Gaillard, Nucl. Phys. **B114**, 334 (1976).
[53]DLS Collaboration, A. Letessier-Selvon *et al.*, Phys. Rev. C **40**, 1513 (1989).
[54]J. Kapusta and P. Lichard, Phys. Rev. C **40**, R1574 (1989).
[55]NA34 (HELIOS) proposal, Report No. CERN-SPS/83-51 (unpublished).
[56]V. Černý, P. Lichard, and J. Pišút, Z. Phys. C **31**, 163 (1986).
[57]P. Lichard, in *Soft Lepton Pair and Photon Production* (Ref. 10).